Analysis of refrigerant mal-distribution
in fin-and-tube evaporators

Kærn, Martin Ryhl; Elmegaard, Brian

Published in:
Danske Køledage

Publication date:
2009

Document Version
Publisher's PDF, also known as Version of record

Citation (APA):
Kærn, M. R., & Elmegaard, B. (2009). Analysis of refrigerant mal-distribution: in fin-and-tube evaporators. In *Danske Køledage: Kompendie* (Vol. 2009, pp. 25-35)

Analysis of refrigerant mal-distribution in fin-and-tube evaporators

Martin Ryhl Kærn[a,b,*], Brian Elmegaard[b]

[a]Automatic Controls, Danfoss A/S
[b]Mechanical Engineering, Technical University of Denmark
[*]Corresponding author: Tel.: +45 7488 2572, e-mail: martin@danfoss.com

Abstract

Refrigerant mal-distribution in fin-and-tube evaporators for residential air-conditioning is investigated numerically in this paper. Essentially the influence of refrigerant mal-distribution on capacity of an evaporator is reported. In order to investigate, a model of a fin-and-tube evaporator is developed in the object-oriented modeling language Modelica. The evaporator model is a dynamic distributed one-dimensional homogeneous model, but will be used here to present results in steady state. Fin-and-tube evaporators usually have a complex circuitry, however the evaporator will be simplified to be two straight tubes. The refrigerant mal-distribution is then induced to the evaporator by varying the vapor quality at the inlet to each tube and the air-flow across each tube. Finally it is shown that mal-distribution can be compensated by an intelligent distributor, that ensures equal superheat temperature in both tubes. The refrigerant is R410a.

Introduction

Energy consumption and refrigerant charge in refrigeration systems are becoming increasingly important for environmental, legislative and economic reasons. Hence compact dry-expansion multi-channel heat exchangers are of interest for future refrigeration technology. The use of more channels in evaporators gives rise to mal-distribution phenomena, which have shown to reduce evaporator capacity and thus system energy efficiency. Refrigerant mal-distribution can be caused by different reasons or interactions of these, such as air-flow mal-distribution, non-uniform air-temperature, fouling, improper heat-exchanger or distributor design and installation.

Several researchers have studied mal-distribution in evaporators and its reducing impact on cooling capacity. Payne and Domanski [1], Lee et al. [2] and Kim et al. [3] studied air-flow mal-distribution, and Nakayama et al. [4], Li et al. [5] studied refrigerant flow distribution in distributors. Particularly Payne and Domanski [1] and Kim et al. [3] demonstrated that individual superheat control of each circuit could recover most of the cooling capacity.

Typically A-coils are employed in residential air-conditioning (RAC) systems as the indoor coil and serves as an evaporator in cooling mode and condenser in heat-pump mode. The coil forms an A-shape in order to reduce the volume of the unit. A drawback is that the air-flow becomes non-perpendicular to the face coil, resulting in air-flow mal-distribution. Models capable of handling user-defined air-flow mal-distribution exists in the literature such as Domanski [6], and Jiang et al. [7]. Recently Domanski and Yashar [8] used computational fluid dynamics (CFD) and particle image velocimetry (PIV) to obtain the air-velocity profile through an A-coil. Likewise AbdelAziz et al. [9] applied CFD to analyze the air-flow in an A-coil. Both showed air-flow mal-distribution.

Domanski and Yashar [8] applies a novel optimization system called ISHED (intelligent system for heat exchanger design) to optimize refrigerant circuitry (tube connections) in order to compensate air-flow mal-distribution. They show that cooling capacity is increased by 4.2% compared to an interlaced type of circuitry.

This study focuses on understanding refrigerant mal-distribution and methods of compensating mal-distribution. The objective is to quantify the influence of the distributor and the air-flow on refrigerant mal-distribution and cooling capacity. The case is ideal, i.e. two straight tubes, in order to perform simple and basic investigation of refrigerant mal-distribution. Finally the hypotheses implied by Payne and Domanski [1] and Kim et al. [3] as mentioned above is investigated, that is "controlling individual superheat temperatures results in recovered capacity at air-side mal-distribution".

Model description

The main assumptions of the distributed model is:

- The refrigerant flow is one-dimensional.
- The refrigerant vapor and liquid are in thermodynamic equilibrium.
- The refrigerant flow is homogeneous.
- The refrigerant kinetic and potential energies are negligible.
- The heat transfer coefficient on the air-side is uniform on each segment.
- The air is dry, incompressible and does not accumulate mass or energy.
- The axial heat conduction of the pipe wall is negligible.
- Heat conduction between each tube is negligible.
- Feeder tube pressure drop negligible.

Further assumptions with regards to the two-phase flow formulation are explained in the following. The inertia term in the momentum equation (the derivative term w.r.t. time) is important for modeling propagation of pressure fluctuations and other effects of very small time scales (see Richter [10]), which is not important in the current study and will be neglected. Also accelerational pressure drop is typically small compared to frictional pressure drop and will also be neglected (see Jiang [11]). The one-dimensional homogeneous two-phase flow formulation for horizontal tubes is then

$$\frac{dM}{dt} = \dot{m}_{in} - \dot{m}_{out} \tag{1}$$

$$\frac{dU}{dt} = (\dot{m}h)_{in} - (\dot{m}h)_{out} + \dot{Q} \tag{2}$$

$$(p_{in} - p_{out}) = \Delta p_f \tag{3}$$

where equation 1, 2 and 3 are the mass conservation, energy conservation and momentum equation. The model has been implemented as described by Jensen [12] and has been verified in steady state by Coil-Designer (Jiang et al. [7]). Additional information needs to be given such as heat transfer coefficient and friction coefficient. The model also includes the thermal mass of the tube wall and employs the effectiveness-NTU relations similar to Jiang [11] for cross-flow heat exchangers. Table (1) gives an overview of the correlations used.

Table 1: Overview of correlations

Air-side	
Heat transfer coefficient	Wang et al. [13]
Fin efficiency	Schmidt [14] (Schmidt approximation)
Two-phase	
Heat transfer coefficient	Shah [15]
Friction coefficient	Müller-Steinhagen and Heck [16]
Single phase	
Heat transfer coefficient	Gnielinski [17]
Friction coefficient	Blasius [18]

Implementation

The model is implemented in Dymola 7.1 [19]. Dymola solvers are able to integrate large scale differential and algebraic equations (DAEs) efficiently. Dymola is based on the Modelica language and supports object-oriented programming, that is important for model reuse and extension. Equations can be written in a casual manner and supports event driven procedures. Dymola has been well tested within the field of air-conditioning and refrigeration (Eborn et al. [20], Richter [10]). Thermophysical properties are provided by the RefEqn package (Skovrup [21]).

A given heat exchanger geometry is chosen within the applicable range of the correlations used, where the considered fin type is louvered. The main input parameters to the model is depicted in table (2).

Table 2: Main input parameters

Distributor pressure, p	10 bar (∼280.5 K)
Distributor inlet quality, x_{in}	0.2
Mean air frontal velocity, $V_m = \frac{V_{fr,1}+V_{fr,2}}{2}$	1.5 m/s
Air temperature, T_{air}	300 K
Tube length, L	7 m
Tube inner diameter, d	7.6 mm
Tube outer diameter, D	9.6 mm
Number of control volumes, n	30 per tube

Now only three boundary conditions are missing. The first is a parameter used for the distributor, that is defined as $F_x = x_{out,2}/x_{in}$. Figure 1 shows a sketch of the model setup including these symbols. When F_x is equal to one, the quality into the evaporator tubes is equal, when F_x is equal to zero, only liquid comes into tube 2. The second is a similar parameter used for the air-flow distribution and is defined as $F_{air} = V_{fr,1}/V_m$. This means: When F_{air} is equal to one, the air-flow is distributed equally across the 2 tubes, when F_{air} is equal to zero, only air travels across tube 2. The third and last boundary condition used is either the overall mass flux (G_{tot} = 358 kg/m^{2}s) or the overall superheat temperature $T_{sh,tot}$ = 5 K. The two give the same result at no mal-distribution. The former serves as a baseline result case (no control of superheat temperature), where the latter reflects the real RAC system (superheat temperature controlled).

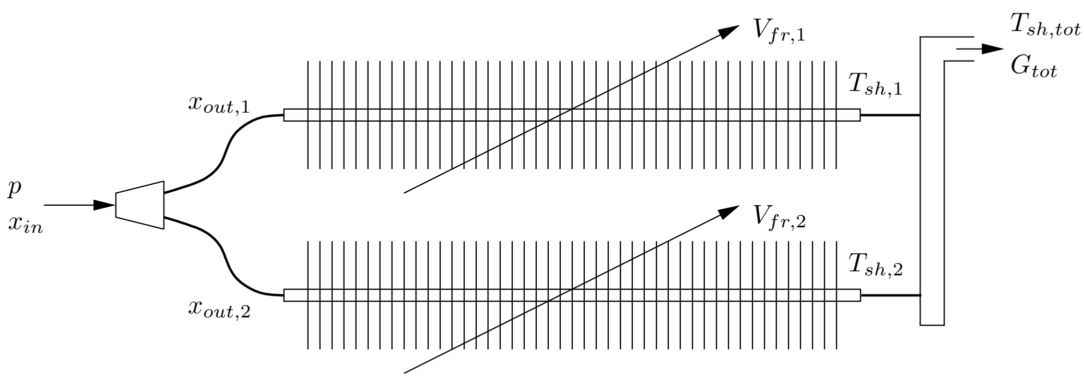

Figure 1: Sketch of model setup

This leads to 4 cases that are investigated. For all cases the thermodynamic state is fixed at the inlet to the distributor. Case 1: F_x is varied from 1 to 0.1, F_{air} is set to 1 and G_{tot} is fixed. Case 2: F_x is varied from 1 to 0.1, F_{air} is set to 1 and $T_{sh,tot}$ is controlled to 5 K by G_{tot}. Case 3: F_x is set to 1, F_{air} is varied from 1 to 0.1 and G_{tot} is fixed. Case 4: F_x is set to 1, F_{air} is varied from 1 to 0.1 and $T_{sh,tot}$ is controlled to 5 K by G_{tot}. Each case is one simulation in Dymola where F_x or F_{air} is varied from 1 to 0.1 and takes about 45 to 60 minutes on a laptop (2.0GHz processer and 2.0GB of RAM).

Results of mal-distribution from the distributor

Figure (2) depicts the mass flux distribution into each tube when the overall mass flux is fixed (case 1).

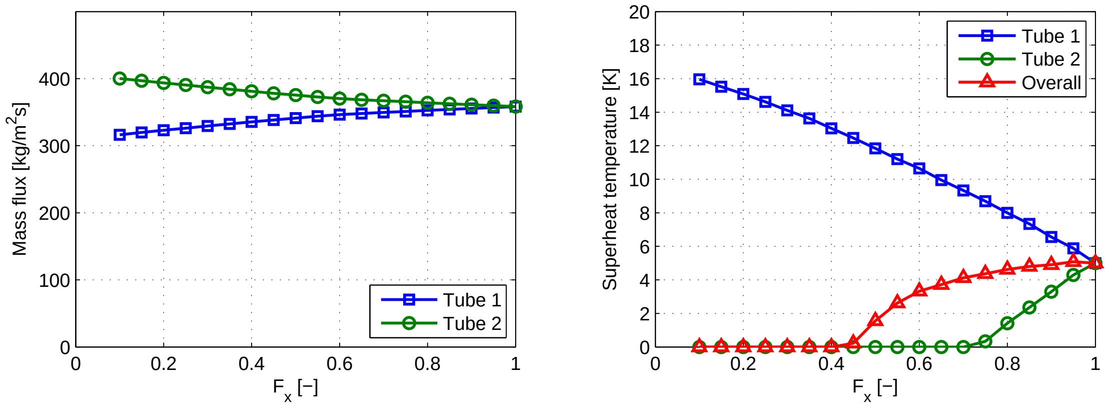

Figure 2: Mass fluxes and superheat temperatures at $G_{tot} = 358$ kg/m^{2}s as function of F_x

It shows that mass flux distribution is dependent on the quality factor F_x, so that more mass comes through the tube with lower inlet quality and less mass comes through the tube with higher inlet quality. This is determined by the pressure drop through each tube that has to be the same. The result of different mass flux is different superheat temperatures out of the tubes as depicted on the right. It shows that liquid comes out of tube 2 at $F_x = 0.7$. The overall superheat temperature is also decreasing as F_x goes to zero, however moderately. This means that capacity is not reduced much, since the overall mass flux is fixed, the evaporator inlet state is fixed and the evaporator outlet superheat is reduced a bit. This can be seen on figure (3), where both tubes capacity is depicted as well as the total capacity.

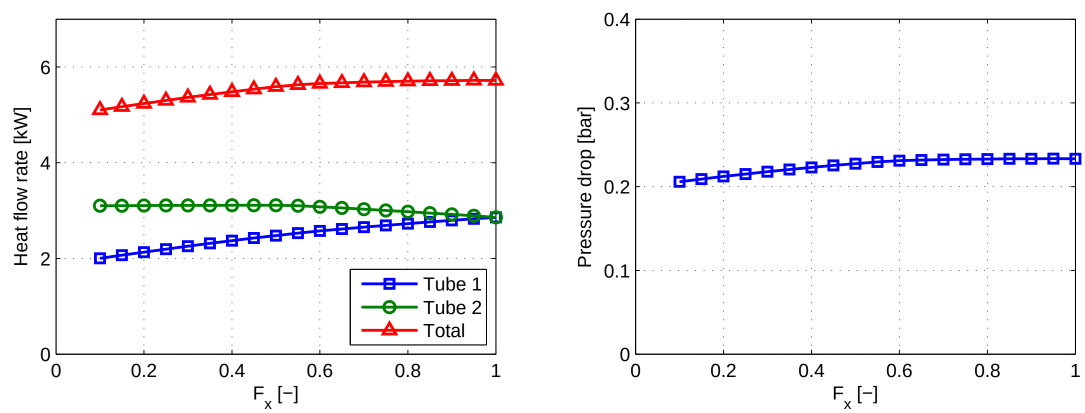

Figure 3: Cooling capacities and pressure drop at $G_{tot} = 358$ kg/m^{2}s as function of F_x

The overall capacity starts to drop slightly when full evaporation is not reached in tube 2. However the capacity of tube 2 becomes higher to the point where full evaporation is not reached. In contrast the capacity of tube 1 becomes smaller because of the higher superheated part. The overall pressure drop tends to become smaller as F_x goes to zero, however not significantly.

In residential air-conditioning systems the overall superheat temperature is normally controlled by a thermostatic expansion valve. This means that this temperature is fixed in steady state.

Figure 4 shows the results at this case (case 2) as F_x goes to zero and compares it to the previous results (case 1).

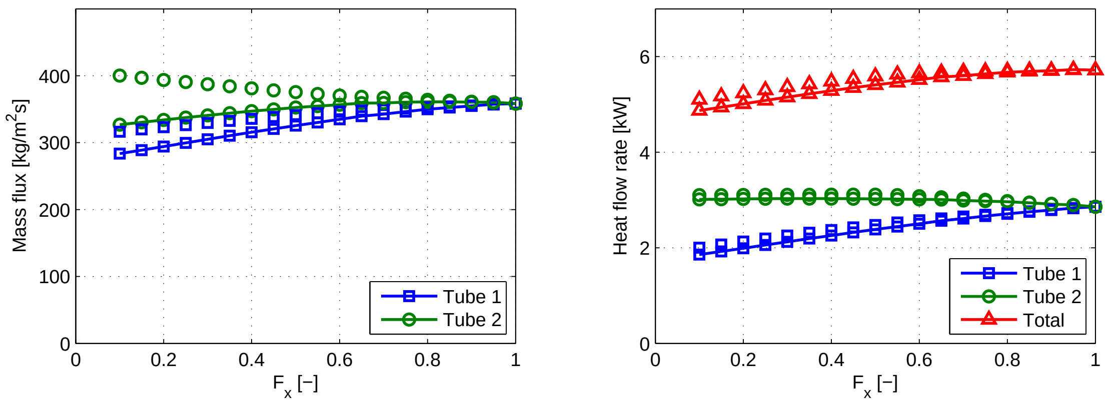

Figure 4: Mass fluxes and heat flows at $T_{sh,tot} = 5$ K as function of F_x. (no line = G_{tot} fixed)

What occurs compared to the previous results, is that the overall mass flux is reduced to maintain the overall superheat. This results in lower mass fluxes for both tubes. Again the mass flux distribution is determined by the pressure drop across each tube that must be the same. The overall heat flow is reduced even more than previously, but not significantly. It is reduced mainly because the overall superheat is controlled to 5 K by reducing the overall mass flux. A minor reduction will also be addressed to the smaller heat transfer coefficient, when the overall mass flux becomes smaller.

The difference between case 1 and 2 is that, for case 1 the capacity drops because of lower overall superheat temperature and for case 2 the capacity drops because of lower overall mass flux.

The overall picture of the influence of mal-distribution from the distributor is the following. In nearly worst case (i.e. $F_x = 0.1$) the capacity is reduced by 11% for fixed overall mass flux and 15% for fixed overall superheat temperature. The results are similar to a study of Brix [22], who showed that cooling capacity in worst case (i.e. $F_x = 0$) is reduced by 13% and 20% in a microchannel type of evaporator. Also the trends on the figures are the same for a microchannel evaporator.

Results of mal-distribution from the air-side

Figure 5 shows the mass flux and cooling capacity distribution as F_{air} goes to zero for both case 3 and 4, i.e. at fixed overall mass flux and fixed overall superheat, respectively.

For fixed overall mass flux, the results show that the refrigerant distribution is significantly influenced by the air-side as F_{air} goes to zero. However for fixed overall superheat temperature the mass flux is distributed almost evenly, but is also reduced significantly. This greatly reduces the cooling capacity, that is lower for fixed overall superheat temperature compared to fixed overall mass flux.

The results show that the mal-distribution of the air-flow (case 3 and 4) reduces the cooling capacity much more significantly than the mal-distributed vapor quality (case 1 and 2). At nearly worst case (i.e. $F_{air} = 0.1$) the capacity is reduced by 46% and 80% for fixed overall mass flux and fixed overall superheat temperature, respectively. Again the results are similar to the trends of Brix [22].

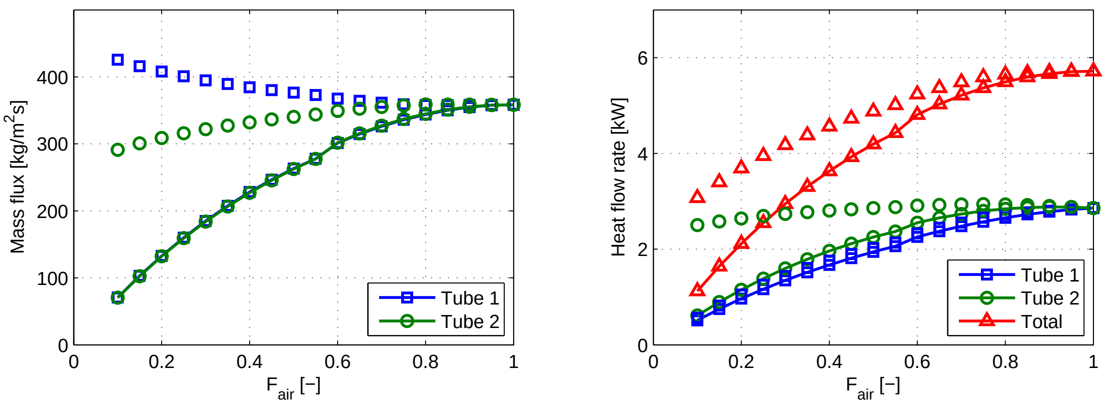

Figure 5: Mass fluxes and heat flows as function of F_{air}. (line = $T_{sh,tot}$ fixed, no line = G_{tot} fixed)

Compensating air-side mal-distribution

It has been shown in the previous section that mal-distribution of air-flow or refrigerant vapor quality reduces the cooling capacity. However if air-side mal-distribution is present, then the refrigerant distribution should be controlled, if possible, to meet the air-side mal-distribution. This is showed in this section, where the individual superheats of the tubes are controlled to 5 K. A pressure drop (degree of freedom) is given to the tube with the smallest pressure drop (tube 2), so that the overall pressure drop is maintained the same across both tubes, allowing for individual control by the mass fluxes. Figure 6 shows the results for the cooling capacity as F_{air} goes to zero and compares it to case 3 and 4.

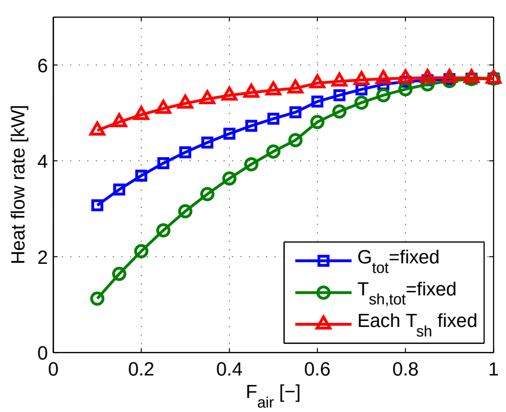

Figure 6: Overall heat flow's as function of F_{air}

It shows that the cooling capacity reduction from the air-side mal-distribution can be significantly recovered by controlling each tube superheat temperature. Kim et al. [3] showed that the cooling capacity could be recovered to 99.9% at $F_{air} = 0.75$. The result of this study show a recovery of 96% at $F_{air} = 0.75$.

Conclusion

It can be concluded that mal-distribution in fin-and-tube evaporators reduces the cooling capacity, whenever it comes from a mal-functioning distributor or a non-uniform air-flow. It turns out that the non-uniform air-side greatly reduces cooling capacity, whereas the mal-functioning distributor does not have that significant impact, when it comes to distribution of vapor quality.

Four cases were studied, i.e case 1 and 2 at mal-distribution from the distributor and case 3 and 4 at mal-distribution from the air-side. Case 1 and 2 showed only 11% and 15% degradation in cooling capacity, respectively, in nearly worst case when F_x is equal to 0.1. Case 3 and 4 showed 46% and 80% degradation in cooling capacity, respectively, in nearly worst case when F_{air} is equal to 0.1. This means that the capacity is reduced about 4 times as much for the non-uniform air-flow compared to non-uniform inlet vapor quality.

The fixed overall mass flux cases (case 1 and 3) showed lower degradation than the fixed overall superheat temperature cases (case 2 and 4).

The overall picture shows that the cooling capacity reduction becomes significant when full evaporation is not reached in one of the tubes. Also air-side mal-distribution can be recovered by controlling individual superheat temperatures.

Further work

Further work is minded on system performance (COP) when mal-distribution is present in the evaporator. Here the mass of refrigerant will be considered in both the evaporator and condenser. This study was carried out at fixed inlet state (pressure and enthalpy), but what happens with e.g. condensing and evaporating pressure, when mal-distribution is present?

The pressure drop in the feeder tubes were not addressed, which could be uneven due to different bend shapes and induce refrigerant mal-distribution.

It is not a fact that controlling the individual superheat temperatures gives the best recovery. One could also control the liquid parts in the tubes to be equal, together with the overall superheat temperature.

This investigation gave rise to another important issue, that is, what is the benefits of optimizing refrigerant circuitry, if refrigerant distribution is controllable and how could the two interact?

References

[1] W. V. Payne, P. A. Domanski, Potential benefits of smart refrigerant distributors, Final report No. ARTI-21CR/610-20050-01, Air-Conditioning and Refrigeration Technology Institute, Arlington, VA, USA (2003).

[2] J. Lee, Y.-C. Kwon, M. H. Kim, An improved method for analyzing a fin and tube evaporator containing a zeotropic mixture refrigerant with air maldistribution, International Journal of Refrigeration 26 (2003) 707–720.

[3] J.-H. Kim, J. E. Braun, E. A. Groll, Analysis of refrigerant flow distribution in evaporators, in: 12th International Refrigeration and Air Conditioning Conference at Purdue, no. 2353, West Lafayette, IN, USA, 2008.

[4] M. Nakayama, Y. Sumida, S. Hirakuni, A. Mochizuki, Development of a refrigerant two-phase flow distributor for a room air conditioner, in: 8th International Refrigeration Conference at Purdue, West Lafayette, IN, USA, 2000, pp. 313–319.

[5] G. Li, S. Frankel, J. E. Braun, E. A. Groll, Application of cfd models to two-phase flow in refrigeration distributors, HVAC&R Research 11 (1) (2005) 45–62.

[6] P. A. Domanski, Finned-tube evaporator model with a visual interface, in: 20th International Congress of Refrigeration, Sydney, Australia, 1999.

[7] H. Jiang, V. Aute, R. Radermacher, Coildesigner: A general-purpose simulation and design tool for air to refrigerant heat exchangers, International Journal of Refrigeration 29 (2006) 601–610.

[8] P. A. Domanski, D. Yashar, Application of an evolution program for refrigerant circuitry optimization, in: ACRECONF "Challenges To Sustainability", New Delhi, India, 2007.

[9] O. AbdelAziz, V. Singh, V. Aute, R. Radermacher, A-type heat exchanger simulation using 2-d cfd for airside heat transfer and pressure drop, in: 12th International Refrigeration and Air Conditioning Conference at Purdue, no. 2200, West Lafayette, IN, USA, 2008.

[10] C. C. Richter, Proposal of new object-oriented equation-based model libraries for thermodynamic systems, Ph.D. thesis, Technische Universität Carolo-Wilhelmina zu Braunschweig, Fakultät für Maschinenbau (2008).

[11] H. Jiang, Development of a simulation and optimization tool for heat-exchanger design, Ph.D. thesis, University of Maryland at College Park, Department of Mechanical Engineering (2003).

[12] J. M. Jensen, Dynamic modelling of thermo-fluid systems with focus on evaporators for refrigeration, Ph.D. thesis, Technical University of Denmark, Department of Mechanical Engineering (2003).

[13] C.-C. Wang, C.-J. Lee, C.-T. Chang, S.-P. Lin, Heat transfer and friction correlation for compact louvered fin-and-tube heat exchangers, International Journal of Heat and Mass Transfer 42 (1999) 1945–1956.

[14] T. E. Schmidt, Heat transfer calculations for extended surfaces, Refrigerating Engineering (1949) 351–357.

[15] M. M. Shah, Chart correlation for saturated boiling heat transfer: Equations and further study, ASHRAE Transactions 88 (1982) 185–196.

[16] H. Müller-Steinhagen, K. Heck, A simple friction pressure drop correlation for two-phase flow in pipes, Chemical engineering and processing 20 (1986) 297–308.

[17] V. Gnielinski, New equation for heat and mass transfer in turbulent pipe and channel flow, International Chemical Engineering 16 (1976) 359–368.

[18] P. R. H. Blasius, VDI Wärmeatlas, 9th Edition, Springer-Verlag, Ch. Lab., 2002.

[19] Dynasim AB, Research Park Ideon SE-223 70, Lund, Sweden, Dynamic Modeling Laboratory, Dymola User's Manual, version 7.1 (2008).

[20] J. Eborn, H. Tummescheit, K. Prölß, Airconditioning - a modelica library for dynamic simulation of ac systems, in: 4th International Modelica Conference, Hamburg, Germany, 2005, pp. 185–192.

[21] M. J. Skovrup, Thermodynamic and thermophysical properties of refrigerants, Department of Energy Engineering, Technical University of Denmark, Nils Koppels Allé, Building 402, DK-2800 Lyngby, Denmark.

[22] W. Brix, Modelling of refrigerant distribution in microchannel evaporators, in: Danske Køledage 2008, 2008, pp. 71–79.